Published in final edited form as:

J Immunol. 2017 July 01; 199(1): 263–270. doi:10.4049/jimmunol.1600409.

SLC46 family transporters facilitate cytosolic innate immune recognition of monomeric peptidoglycans

Donggi Paik[*], **Amanda Monahan**[*], **Daniel R. Caffrey**[*], **Roland Elling**[*], **William E. Goldman**[†], and **Neal Silverman**[*]

[*]Program in Innate Immunity, Division of Infectious Diseases and Immunology, Department of Medicine, University of Massachusetts Medical School, 364 Plantation Street, Worcester, Massachusetts, 01605 USA

[†]Department of Microbiology and Immunology, University of North Carolina at Chapel Hill, Chapel Hill, North Carolina, 27599 USA

Abstract

Tracheal Cytotoxin (TCT), a monomer of DAP-type peptidoglycan (PGN) from *B. pertussis*, causes cytopathology in the respiratory epithelia in mammals and robustly triggers the *Drosophila* Imd pathway. PGRP-LE, a cytosolic innate immune sensor in *Drosophila*, directly recognizes TCT and triggers the Imd pathway, yet the mechanisms by which TCT accesses the cytosol are poorly understood. In this study, we report that CG8046, a *Drosophila* SLC46 family transporter, is a novel transporter facilitating cytosolic recognition of TCT, and CG8046 plays a crucial role in protecting flies against systemic *E. coli* infection. In addition, mammalian SLC46A2s promote TCT triggered NOD1 activation in human epithelial cell lines, indicating that SLC46As are a conserved group of PGN transporters contributing to cytosolic immune recognition.

Introduction

Fragments of PGN are strong activators of innate immune responses in both mammals and insects. In mammals, γ-D-Glu-meso-DAP, a dipeptide derivative from DAP-type PGN, is the minimal activator of NOD1. On the other hand, muramyl dipeptide (MDP), a monosaccharide dipeptide derived from either Lysine-type or DAP-type PGNs, activates NOD2. Both these NOD receptors trigger NF-κB and MAPK signaling pathways, driving production of proinflammatory cytokines and chemokines (1). In addition, NLRP1 and NLRP3 form inflammasome complexes in response to MDP (2, 3). TCT is a monomer of DAP-type PGN released by *Bordetella pertussis* and *Neisseria gonorrhoeae* and known to cause massive cell death in ciliated epithelia in mammals as well as to activate *Drosophila* innate immune responses (4, 5).

In *Drosophila*, the PGN recognition proteins (PGRPs) directly recognize PGN and trigger either of the two major *Drosophila* immune response pathways, Toll and Imd, culminating in robust induction of antimicrobial peptides (6–8). Among 13 PGRPs in *Drosophila,* PGRP-

Corresponding author: Dr. Neal S. Silverman, Phone; 508-856-5826, Fax; 508-856-5463, Neal.Silverman@umassmed.edu.

LC and PGRP-LE bind specifically to DAP-type PGN and trigger the Imd pathway. PGRP-LC is a transmembrane protein that recognizes both polymeric DAP-type PGN and monomeric TCT in the extracellular milieu, whereas PGRP-LE senses TCT in the cytosol (9). However, the molecular mechanisms by which TCT accesses the cytosol to be sensed by PGRP-LE have not been explored.

In this study, we examine the delivery of TCT to the cytosolic PGN receptors PGRP-LE in *Drosophila* and NOD1 in mammals. *Drosophila* SLC15 homologs, which have been previously associated with transport of Tri-DAP (NOD1 agonist) and MDP (NOD2 agonist), did not facilitate TCT recognition in *Drosophila*. On the other hand, a targeted RNAi screen identified CG8046, a *Drosophila* SLC46 as a novel transporter facilitating cytosolic recognition of TCT. We further show that mammalian SLC46As also facilitate TCT and MDP triggered NOD receptor activation in human epithelial cells.

Materials and Methods

Cell culture

Drosophila S2* cells were maintained in Schneider's *Drosophila* media (Gibco) supplemented with 10 % FBS, 1 % GlutaMAX (Gibco) at 27 °C. HEK293 cells were maintained in DMEM (Corning CellGro) supplemented with 10 % heat-inactivated FBS at 37 °C, 5 % CO_2. HCT-116 cells (ATCC) were maintained in McCoy's 5A (Iwakata & Grace Modification, Corning CellGro) supplemented with 10 % heat-inactivated FBS at 37 °C, 5 % CO_2.

Live-Imaging of HEK293 cells

HEK293 cells were seeded in DMEM (Corning CellGro) supplemented with 10% heat-inactivated FBS on Nunc Glass Bottom Dishes (Thermofisher) coated with Poly-L-Lysine (Sigma) for 24 h at 37 °C (50,000 cells/plate). Cells were transfected with pEF-Slc46a2-EGFP-V5 construct using GeneJuice Transfection Reagent (Millipore) and OptiMEM media (Gibco), per manufacturer's instructions. Transfected cells were kept at 37°C for 24 h. To label the late endosomes and lysosomes, 20uL of 10 μM LysoTracker (Thermofisher) was added to each dish and cells were incubated at 37 °C for 30 min in the presence or absence of 10 μM TCT. After incubation, media was removed and cells were washed twice with HBSS (Corning CellGro) and immersed in HBSS for imaging. Imaging was performed using a Leica TCS SP8. To measure the perimeter of the SLC46A2-EGFP-expressing, LysoTracker-positive puncta, Z-stacks of optical sections spanning each individual cell were acquired, and the focal point with the greatest surface area per puncta was measured. Each representative image was generated with 3–5 optical sections that were reconstructed into 3D images and flattened into the 2D. All images were acquired on the same day, using the same microscope settings and exposure times FIJI/ImageJ and Adobe Photoshop CS6 were utilized to process and format images.

RNAi

For qRT-PCR, $1X10^6$ S2* cells were plated in 1 ml media and transfected with 2 μg of dsRNA using calcium phosphate method the following day. For western blotting, $1X10^7$ S2*

cells were transfected with 20 μg of dsRNA. In both cases, cells were split into 1:3 in fresh medium 48 hours after transfection and treated with 1 μM 20-hydroxyecdysone for 24 hours before stimulation. All the RNAi target sequences were retrieved from Harvard DRSC/TRiP Functional Genomics Resources (www.flyrnai.org). For RNAi in human epithelial cell lines, 20,000 cells were co-transfected with 5 pmole of ON-TARGETplus Human NOD1 siRNA - SMARTpool or ON-TARGETplus Non-Targeting Pool (Dharmacon) and plasmids in a 96-well plate using Lipofectamine 2000 (Invitrogen).

qRT-PCR

Total RNA was isolated with Trizol (Invitrogen). 0.5 μg of total RNA was treated with amplification grade DNaseI (Invitrogen) and used for cDNA synthesis (iScript cDNA synthesis kit, BioRad). SYBR Green Supermix (BioRad) was used for real-time PCR using diluted 1st strand cDNA. PCR primer sequences are as follow: GAPDH1_fw; ATCGTCGAGGGTCTGATGAC, GAPDH1_rev; CGGACGGTAAGATCCACAAC, Dpt_fw; TAGGTGCTTCCCACTTTCCA, Dpt_rev; CATTGCCGTCGCCTTACTT, yin_fw; AATGAGTTCTGCGAGCGATT, yin_rev; TCCCGATCGCAATTAGTAGG, CG2930_fw; CCAGCGAGTTCTTCCTGTTC, CG2930_rev; CTTGCCCTTGTTCTCGACTC, CG9444_fw; GGCAATCTGATCGTGGTTCT, CG9444_rev; TGTAATCGAAGGCCAAAAGG, CG8046_fw; CTGTGCCATGTACACCCAAG, CG8046_rev; AGCCACGGAATAGGTCACAC. All the experiments were repeated at least twice.

Dual-Luciferase reporter assay

For *Attacin A*-luciferase assay, 1X10^5 S2* cells were plated in 96-well plate and transfected with 50 ng of *Attacin A*-luciferase (10), 5 ng of p*Copia*-Renilla luciferase and 50 ng of pAc5.1 plasmid using Effectene (Qiagen) for 48 h. For NF-kB luciferase assay, 20,000 cells (HEK293 or HCT-116) were plated in 96-well plate and transfected with 50 ng NF-kB luciferase, 5 ng of pRL-TK (Promega) and 5 ng of pEF plasmid using GeneJuice (Millipore) for 24 h. In all cases, cells were stimulated with indicated ligands for 6 h and subject to dual-luciferase assay. All transfections were performed in triplicates and relevant firefly luciferase activity was normalized to *Renilla* luciferase activity. All the experiments were repeated at least twice.

Statistics

All the statistical analyses were performed using GraphPad Prism. 2-way ANOVA followed by Tukey's multiple comparison or unpaired two-tailed t-test was used as indicated. Standard deviation was presented as an estimate of variation. *P* values of <0.05 were considered significant. For survival experiment, log-rank test was used for statistical analysis.

Western blotting

For Imd protein cleavage experiment, 50 μg of total protein from whole lysate was separated by SDS-PAGE (10 % acrylamide gel) and immunoblotted with anti-Imd antibody (11). After

probing with anti-Imd antibody, the blot was stripped and reprobed with chicken anti-GFP antibody (Abcam, ab13970) to detect YFP-PGRP-LE.

Drosophila genetics

To generate deletion mutants for *yin*, pBac{WH}*roX1*[f07388] (Exelixis Collection at Harvard University), P{XP}*yin*[d02176] (Bloomington Drosophila Stock Center, No. 19172), and hs-FLP (Bloomington Drosophila Stock Center, No. 279) were used to induce FRT/FLP mediated recombination as previously described (12). Male progenies were screened for loss of *mini-white* marker resulting from recombination between 2 transposons and 3 positive hits were recovered and balanced. All mutants were homozygous-viable and fertile. Genomic DNA PCR confirmed resulting hybrid elements.

Deletion mutants for *CG8046* were generated by homology-directed repair combined with CRISPR-Cas9 method. 2 guide sequences targeting both 5′ upstream and 3′ downstream regions of *CG8046* coding DNA sequence were selected and cloned into pCFD4 vector (Addgene Plasmid #49411) (AACTCAACTGAGTCTTGAAA for 5′, GGTTTTTAAATGATTTATGG for 3′). pCFD4 harboring 2 guide RNA sequences and pHD-DsRed plasmid (Addgene Plasmid #51434) with homology arms flanking 3XP3 DsRed transgene were co-injected into w^{1118}; PBac{*y*[+mDint2]=*vas-Cas9*}VK00027 strain (Bloomington Drosophila Stock Center, No. 51324). Injected animals were crossed to w^{1118} strain and male progeny were screened for eye-specific DsRed expression. Over 20 DsRed-positive hits were recovered and balanced. Genomic DNA PCR and RT-PCR further confirmed deletion of *CG8046* locus.

For *in vivo* overexpression assays, a *PGRP-LC* knockdown strain was generated first with a transgene for *PGRP-LC* RNAi (Vienna Drosophila Resources Center, No. 51968) and the C564 Gal4 driver in a single stock (13). This line failed to induce robust *Diptericin* induction upon challenge with *E.coli,* as expected. EP elements driving expression of *CG8046* (Bloomington Drosophila Stock Center, No. 27107) or *CG30344* (Bloomington Drosophila Stock Center, No. 28425) were crossed to PGRP-LC knockdown strain and resulting progenies were analyzed for *Diptericin* induction by qRT-PCR following TCT injection (9).

E. coli Infection and Survival Experiments

E. coli 1106 was grown overnight in LB-broth at 37 °C to an O.D. of 2.0 and was pelleted. Flies were pricked with a needle inoculated with *E. coli 1106* or clean pricked (as a control). Infections were administered between the haltere and wing joint in the metathorax of flies aged 3–7 days. Flies were kept at 25 °C over the course of the experiment. Survival was measured every 24 h. Seven independent survival experiments were performed and one representative result is presented in this report.

Flow cytometry

All SLC46 and SLC15 expression constructs are C-terminally fused to V5 tag and in order to check their expression, transfected cells were treated with trypsin/EDTA to obtain single cell suspension. After fixation and permeabilization using FoxP3 staining buffer set (eBioscience), V5 tag was stained with anti-V5-FITC or anti-V5-Alexa647 (Invitrogen) in

1X Permeabilization buffer. LSR II (BD Biosciences) and FlowJo (Tree Star) were used for flow cytometry and analysis. Dead cells were excluded using the Live/dead fixable aqua dead cell stain kit (Invitrogen). Live, singlet cells were gated for detection of V5 tag.

Bioinformatics

Sequences were retrieved from Ensembl and aligned with Clustal Omega version 1.2.0 (14). Phylogenetic trees were reconstructed using the neighbor-joining method and BLOSUM 50 matrix in PFAAT version 2 (15). To assess the reliability of internal nodes, the bootstrap method was performed for 1000 replicates and displayed as a percentage on each node. We confirmed that these neighbor-joining trees had the same topologies as the corresponding gene trees in Ensembl, which are based on a maximum likelihood method.

Results

SLC15s are not associated with cytosolic recognition of TCT in *Drosophila*

Earlier studies have suggested that members of Solute Carrier 15 (SLC15) family facilitate translocation of NOD1 and NOD2 agonists into epithelial cells as well as in dendritic cells (16–20). Interestingly, Yin, a *Drosophila* SLC15 identified in *Drosophila* S2* cell phagosome, was reported to enhance MDP recognition in human embryonic kidney (HEK) 293 cells (21). Therefore, we first generated a deletion allele of *yin* to determine if Yin is required for TCT triggered activation of the cytosolic PGN receptor PGRP-LE. However, TCT still triggered robust systemic *Dpt* induction in *PGRP-LC, yin* double mutants (Supplemental Figure 1A through D). Note that PGRP-LC was eliminated in this experimental design to force all recognition through the cytosolic PGRP-LE-dependent pathway.

In order to facilitate further studies, we established an S2* cell-based assay. Since PGRP-LE expression is very low in S2* cells, *Diptericin* induction in response to TCT is completely *PGRP-LC* dependent (Figure 1A) (5). To ask if S2* cells have TCT transporter activity, S2* cells were transfected with an *Attacin A* (*AttA*)-luciferase reporter and expression plasmids for different *PGRP-LE* alleles, including wild type and three point mutants. These mutants were previously shown to interrupt TCT binding and/or TCT-induced multimerization (22). Wild type PGRP-LE significantly promoted *AttA*-luciferase activity in response to TCT, but the mutant alleles failed to do so (Figure 1B). This data indicates that S2* cells can transport TCT across the plasma membrane for cytosolic recognition by PGRP-LE.

Based on this result, a stable S2* cell line expressing YFP-tagged PGRP-LE (PGRP-LE stable cells hereafter) was established. When PGRP-LC was knocked down, PGRP-LE stable cells failed to induce *Dpt* upon polymeric PGN stimulation, but continued to respond to TCT, albeit somewhat reduced, in an *imd* and *Relish* dependent manner (Figure 1C). Together these data demonstrate that S2* cells are capable of transporting TCT to the cytosol for detection by PGRP-LE, and we reasoned that double knockdown of PGRP-LC and potential TCT transporters should make PGRP-LE cells less responsive to TCT stimulation.

As earlier studies suggested SLC15s function as Tri-DAP and MDP transporters, all three *Drosophila* SLC15s were tested for their potential role in TCT transport in this cell-based assay (Supplemental Figure 1E). Although all three *Drosophila* SLC15s were readily detectable and subject to efficient knockdown by RNAi, these transporters were not individually or jointly required for TCT activation of the cytosolic PGRP-LE pathway (Supplemental Figure 1F through O). Furthermore, *AttA*-luciferase assay revealed that transient expression of *Drosophila* SLC15s did not enhance TCT-stimulated reporter activity (Supplemental Figure 1P to R). Therefore, we concluded that *Drosophila* SLC15s are not associated with cytosolic recognition of TCT.

A *Drosophila* SLC46 homolog supports cytosolic TCT recognition

As the phagosome is the site of microbial degradation, PGN transporters are likely to be localized to this compartment. Therefore, we next focused on candidate transporters associated with the S2* cell phagosome (Figure 2A) (21). In particular, SLCs, rather than ABC transporters, are typically linked to solute influx in eukaryotic cells (23, 24). PGRP-LC as well as each of 5 additional SLC transporters were silenced in PGRP-LE stable cells. RNAi of either JhI-21 or CG8046 caused a ~10-fold decrease in *Dpt* induction in response to TCT, suggesting that these two transporters may be associated with TCT/PGRP-LE pathway (Figure 2B). To determine if the decrease in *Dpt* induction was specific to the TCT/PGRP-LE pathway, JhI-21 or CG8046 were knocked down while PGRP-LC was left intact. In this case, *JhI-21* RNAi still significantly impaired *Dpt* induction in response to either TCT or polymeric PGN, whereas *CG8046* RNAi did not (Figure 2C). These results argue that CG8046 functions specifically in the cytosolic TCT/PGRP-LE pathway, while JhI-21 has a more general role in regulating the Imd pathway or S2* cell physiology. To validate this finding, an independent dsRNA targeting a different region of CG8046 was synthesized. Again, double knockdown of CG8046 and PGRP-LC severely blocked *Dpt* induction (~12-fold decrease) upon TCT stimulation, while CG8046 single knockdown had no effect (Figure 2D). Knockdown efficiency of CG8046 was greater than 60%, and expression of *CG8046* was immune-inducible (Figure 2E).

The most receptor proximal signaling event characterized in the Imd pathway is the rapid proteolytic cleavage of Imd by the *Drosophila* Caspase-8 homolog Dredd (25, 26). In PGRP-LE stable cells treated with either LacZ or PGRP-LC RNAi, TCT induced robust Imd cleavage as expected. However, when both PGRP-LC and CG8046 were depleted, TCT-induced cleavage of Imd was lost (Figure 2F, top). CG8046 RNAi did not change YFP-PGRP-LE protein level (Figure 2F, bottom). These results demonstrate that CG8046 participates in the activation of the Imd pathway upstream of receptor associated Imd cleavage, further supporting the model that CG8046 functions prior to the interaction of TCT with PGRP-LE as expected for a TCT transporter. Altogether, these results imply that CG8046 is a TCT transporter in *Drosophila*.

Phylogenetic analyses indicated that CG8046 is one of 8 *Drosophila* homologs of SLC46A transporters (Figure 3A). To further analyze the activity of CG8046 in comparison with other paralogs, the *AttA*-luciferase assay was performed in PGRP-LE stable cells transiently expressing each of 8 *Drosophila* SLC46 paralogs. Expression of CG8046 had the most

robust effect on TCT-stimulated *AttA* reporter activity, with a ~2.3-fold increase (Figure 3B, empty vector vs CG8046, 1 μM TCT, P<0.0001). With the exception of CG15553, expression of CG8046 and other SLC46s was robust in these S2* transfection assays (Supplemental Figure 2A and B), suggesting that among these 7 SLC46s, only CG8046 has the ability to deliver TCT to the cytosol. However, CG15553 expression was very weak, and CG15553 is not naturally expressed in S2* cells. Therefore, the ability of CG15553 to transport TCT is unknown.

CG8046 supports cytosolic TCT recognition *in vivo* and plays an important role in host defense against systemic gram-negative infection

Next, the role of CG8046 in recognition of TCT was investigated *in vivo. CG8046* was overexpressed in the fat body while simultaneously silencing PGRP-LC with a hairpin RNA, using the *C564* Gal4 driver. The resulting flies were challenged by TCT injection. *Diptericin* expression was significantly higher in animals with overexpressed *CG8046* compared to the control animals at 6 hours after injection (Figure 3C and D). For comparison, *CG30344*, another SLC46 paralog which showed no activity when expressed in S2* cells, was similarly overexpressed in flies. In this case, *Diptericin* induction was lower following TCT challenge. These results confirm that CG8046 is sufficient to promote TCT recognition by PGRP-LE in adult flies as well as S2* cells.

To further characterize the role of CG8046 *in vivo*, we generated a null allele of CG8046 by CRISPR/Cas9. Upon injection with TCT, the double *PGRP-LC*, *CG8046* mutant adult flies exhibited robust systemic induction of *Dpt* (Supplemental Figure 2C–F). However, Malpighian tubules, the highly immune responsive *Drosophila* renal system (27), failed to respond to response to TCT challenge (p<0.0001), in the double *PGRP-LC*, *CG8046* mutant flies (Figure 3E). Notably, modEncode data suggest that CG8046 is only weakly expressed in the Malpighian tubule (28), however, it is immune-inducible and readily detectable in this tissue, as in S2* cells, after immune challenge (Supplemental Fig. 2G). In addition, the *PGRP-LC, CG8046* double mutant flies succumbed to systemic *E. coli* infection as observed in the *PGRP-LC, PGRP-LE* double mutant (Figure 3F). This finding suggests that CG8046 is a critical component of PGRP-LE-dependent cytosolic host defense. Altogether, these results suggest that CG8046 supports cytosolic recognition of monomeric PGN *in vivo,* in the Malpighian tubules*,* and plays an essential role for protection against certain systemic gram-negative infection. Our results also imply that *Drosophila* may use redundant mechanisms for the cytosolic import of TCT, and the roles of specific transporters may vary depending on the tissue.

Mammalian SLC46A transporters facilitate NOD1 signaling

Next, we asked whether human and mouse SLC46 transporters also promote TCT recognition. To this end, NF-κB luciferase assays were performed in HEK293 cells, which express a low but functional amount of NOD1. The SLC46 transporter family has 3 paralogs in mice and humans (Figure 3A). SLC46A1/proton-coupled folate transporter is responsible for the intestinal absorption of folate and antifolates (29). SLC46A2/TSCOT was first identified because of its abundant expression in mouse thymic cortical epithelial cells, but has not been functionally characterized (30). Likewise, SLC46A3 is not yet characterized.

Expression of human SLC46A2 resulted in a ~4.6-fold increase (empty vector vs hSLC46A2, $p < 0.000$;1) in NF-κB reporter activity in response to TCT. Mouse Slc46a2 also showed significant increase in TCT-triggered NF-κB reporter activity (Figure 4A). All six mammalian transporters were robustly expressed in transfected HEK293 cells, as monitored by FACS (Figure 4B & C). HCT-116, a human colorectal cancer cell line, also showed enhanced responses to TCT, with either human or mouse SLC46A2 as well as with mouse Slc46a3 (Figure 4D). Expression of SLC46 transgenes was comparable except human SLC46A3, which was significantly lower in HCT-116 cells (Figure 4E & F). Therefore, we could not draw any conclusion on the activity of hSLC46A3 in the HCT-116 assays.

Next, we tested if the SLC46 transporters also facilitate recognition of MDP, a NOD2 agonist. Similar dual-luciferase assays were repeated in HCT-116 cells and the same SLC46 homologs that promoted TCT recognition also enhanced NF-κB activation in response to MDP (Figure 4G). These results suggest that members of SLC46 family are conserved transporters for muropeptides in general.

The enhanced NF-κB activation observed in response to TCT was not observed with expression of SLC15A1, SLC15A2 or SLC15A4, which were previously associated with Tri-DAP and MDP uptake (Figure 4H & I) (18, 20, 21). On the other hand, SLC46A2 did not enhance the response to TNF, which indicates that SLC46A2 does not generally enhance NF-κB activation (Figure 4J).

NOD1 and NOD2 signal through RIP2 kinase to activate the MAPK and the IKK signaling pathways. To determine if NF-κB activation supported by SLC46 and TCT is NOD1-dependent, NOD1 was silenced by siRNA in HEK293 cells expressing human SLC46A2. NF-κB luciferase assays showed that NOD1 RNAi significantly decreased NF-κB activation compared to the non-targeting siRNA upon TCT stimulation (Figure 4K). Next, HEK293 cells expressing SLC46A2 were stimulated with TCT and TNF in the absence or presence of gefitinib, an effective RIP2 tyrosine kinase inhibitor (31). NF-κB activation supported by SLC46A2 and TCT decreased with increasing concentrations of gefitinib in a dose-dependent manner, while there was no effect on TNF stimulation (Figure 4L).

Lastly, the subcellular localization of SLC46A2 was examined in HEK293 cells. Confocal microscopy revealed that mouse Slc46a2-EGFP was localized to acidic subcellular organelles labeled by LysoTracker and distributed evenly throughout the cytoplasm without TCT (Figure 5A). However, upon exposure to TCT, mSlc46a2-EGFP-expressing LysoTracker-positive organelles aggregated to form, in significant quantities, large LysoTracker-positive clusters in the cytosol (Figure 5B and C). Human SLC46A2-EGFP behaved similarly, forming large LysoTracker-positive clusters in response TCT (Figure 5D). These data suggest that SLC46A2 facilitates NF-κB activation triggered by NOD1/RIP2 in response to TCT from acidic organelles, most likely late-endosomes and/or endolysosomes, in human cells.

Discussion

Notwithstanding that mammalian NOD1 and *Drosophila* PGRP-LE lack any sequence homology, both receptors promote cytosolic recognition of monomeric DAP-type PGNs, like TCT, and trigger conserved NF-κB signaling pathways leading to profound changes in target gene expression. By applying a targeted RNAi approach in engineered S2* cells, we identified CG8046, a *Drosophila* SLC46 family transporter, as a putative TCT transporter. In S2* cells, knockdown of CG8046 profoundly hampered PGRP-LE-mediated recognition of TCT including downstream signaling events as well as AMP gene induction. On the other hand, overexpression of CG8046 enhanced responses to TCT in S2* cells and adult flies. A *CG8046* deletion allele exhibited normal activation of the intracellular TCT/PGRP-LE pathway in adult flies at systemic level, which is primarily fat body mediated. However, the Malpighian tubules significantly relied on CG8046 for robust induction of *Dpt* upon cytosolic TCT stimulation, and mutant adult flies lacking both *PGRP-LC* and *CG8046* succumbed to *E. coli* infection similar to *PGRP-LC* and *PGRP-LE* double mutants. Our results argue that *Drosophila* utilizes redundant mechanisms to present TCT to the cytoplasmic receptor PGRP-LE, and the relative contribution of the redundant transporters varies between different tissues; CG8046 is a major component of this pathway in at least in the Malpighian tubules as well as hemocyte-derived S2* cells, but plays little role in the fat body.

In our efforts to determine the functional relevance of human SLC46A2 in innate immune recognition, we examined a number of cell lines, including HEK293T, HCT-116, HT-29, THP-1, and MCF-7, but SLC46A2 was negligible in all, making loss of function analysis impractical. *In vivo,* expression of human SLC46A2 is highest in thymus, similar to the mouse ortholog (data not shown) (30). With no published information on the role of NLRs in thymic function, it is not yet possible to postulate the role of SLC46A2 in this tissue. Publicly available database (http://biogps.org/) further indicated that human and mouse SLC46A2 are commonly expressed in skin. In addition, human, but not mouse, CD14-positive monocytes, endometrium and lung also show moderate SLC46A2 expression. Human keratinocytes express SLC46A2 and respond to NOD1 agonist (32). Therefore, keratinocytes are of primary interest to further characterize the role of SLC46A2 in human cells.

Previously, Magalhaes *et al.* (2005) suggested that mouse Nod1, but not human NOD1, recognized TCT based on their dual-luciferase assays where human or mouse NOD1 and TCT were co-transfected into HEK293 cells (33). However, our data argue that human NOD1 is a sensitive sensor of TCT, but requires SLC46A2 for proper delivery of TCT to this endogenous cytosolic receptor (Figure 4).

The human genome encodes over 390 SLC proteins (347 SLCs in *Drosophila*) that are grouped into 52 families (24, 34). Although both SLC15 family and SLC46 family are proton-driven cotransporters, they are distantly related. While SLC15 family members have been described to transport oligopeptides and amino acids, SLC46A1, the founding member of SLC46 family has been reported to transport folic acid and its derivatives, and heme with lower affinity. In fact, the SLC46 family is most similar in its major facilitator superfamily

(MFS) fold with SLC2, SLC16, SLC17, SLC18, SLC22, SLC37, SLC43 and SLCO, which are organic ion transporters based on their sequences (35), but not SLC15. Nonetheless, some of the SLC46s, in flies and mammals, appear to promote the delivery and recognition of muropeptides. The overlapping, but distinct expression pattern of these SLC46s may allow the host to perform optimal surveillance for pathogens as well as commensals in different tissues.

Supplementary Material

Refer to Web version on PubMed Central for supplementary material.

Acknowledgments

The authors thank Anni Kleino for critical reading of the manuscript, Maninjay Atianand for technical assistance and discussion, Jean Luc Imler for *Attacin A*-luciferase construct, Stephen Girardin for SLC15A4 construct, and Michael Brodsky for gene editing by CRISPR.

This work was supported by grants from US National Institutes of Health (RO1 AI060025 to N.S., Ruth L. Kirschstein NIH/NIGMS T32-CA-130807-08 to A.M.) and Mizutani Foundation for Glycoscience (Japan, Grant No. 150183 to N.S.). Stocks obtained from the Bloomington Drosophila Stock Center (NIH P40OD018537) were used in this study.

Abbreviation

Dpt	*Diptericin*
dsRNA	double stranded RNA
PGN	peptidoglycan
TCT	tracheal cytotoxin

References

1. Caruso R, Warner N, Inohara N, Núñez G. NOD1 and NOD2: Signaling, Host Defense, and Inflammatory Disease. Immunity. 2014; 41:898–908. [PubMed: 25526305]
2. Chavarría-Smith J, Vance RE. The NLRP1 inflammasomes. Immunol Rev. 2015; 265:22–34. [PubMed: 25879281]
3. Martinon F, Agostini L, Meylan E, Tschopp J. Identification of bacterial muramyl dipeptide as activator of the NALP3/cryopyrin inflammasome. Curr Biol. 2004; 14:1929–1934. [PubMed: 15530394]
4. Wilson R, Read R, Thomas M, Rutman A, Harrison K, Lund V, Cookson B, Goldman W, Lambert H, Cole P. Effects of Bordetella pertussis infection on human respiratory epithelium in vivo and in vitro. Infect Immun. 1991; 59:337–345. [PubMed: 1987048]
5. Kaneko T, Goldman WE, Mellroth P, Steiner H, Fukase K, Kusumoto S, Harley W, Fox A, Golenbock D, Silverman N. Monomeric and Polymeric Gram-Negative Peptidoglycan but Not Purified LPS Stimulate the Drosophila IMD Pathway. Immunity. 2004; 20:637–649. [PubMed: 15142531]
6. Valanne S, Wang JH, Rämet M. The Drosophila Toll Signaling Pathway. The Journal of Immunology. 2011; 186:649–656. [PubMed: 21209287]
7. Kurata S. Peptidoglycan recognition proteins in Drosophila immunity. Dev Comp Immunol. 2014; 42:36–41. [PubMed: 23796791]
8. Kleino A, Silverman N. The Drosophila IMD pathway in the activation of the humoral immune response. Dev Comp Immunol. 2014; 42:25–35. [PubMed: 23721820]

9. Kaneko T, Yano T, Aggarwal K, Lim JH, Ueda K, Oshima Y, Peach C, Erturk-Hasdemir D, Goldman WE, Oh BH, Kurata S, Silverman N. PGRP-LC and PGRP-LE have essential yet distinct functions in the drosophila immune response to monomeric DAP-type peptidoglycan. Nat Immunol. 2006; 7:715–723. [PubMed: 16767093]
10. Tauszig S, Jouanguy E, Hoffmann JA, Imler JL. Toll-related receptors and the control of antimicrobial peptide expression in Drosophila. Proceedings of the National Academy of Sciences. 2000; 97:10520–10525.
11. Chen L. TAK1-Mediated Post-Translational Modifications Modulate Immune Response: A Dissertation. 2015
12. Parks AL, Cook KR, Belvin M, Dompe NA, Fawcett R, Huppert K, Tan LR, Winter CG, Bogart KP, Deal JE, Deal-Herr ME, Grant D, Marcinko M, Miyazaki WY, Robertson S, Shaw KJ, Tabios M, Vysotskaia V, Zhao L, Andrade RS, Edgar KA, Howie E, Killpack K, Milash B, Norton A, Thao D, Whittaker K, Winner MA, Friedman L, Margolis J, Singer MA, Kopczynski C, Curtis D, Kaufman TC, Plowman GD, Duyk G, Francis-Lang HL. Systematic generation of high-resolution deletion coverage of the Drosophila melanogaster genome. Nature genetics. 2004; 36:288–292. [PubMed: 14981519]
13. Harrison DA, Binari R, Nahreini TS, Gilman M, Perrimon N. Activation of a Drosophila Janus kinase (JAK) causes hematopoietic neoplasia and developmental defects. EMBO J. 1995; 14:2857–2865. [PubMed: 7796812]
14. Sievers F, Wilm A, Dineen D, Gibson TJ, Karplus K, Li W, Lopez R, McWilliam H, Remmert M, Soding J, Thompson JD, Higgins DG. Fast, scalable generation of high-quality protein multiple sequence alignments using Clustal Omega. Mol Syst Biol. 2011; 7:539. [PubMed: 21988835]
15. Caffrey DR, Dana PH, Mathur V, Ocano M, Hong EJ, Wang YE, Somaroo S, Caffrey BE, Potluri S, Huang ES. PFAAT version 2.0: a tool for editing, annotating, and analyzing multiple sequence alignments. BMC Bioinformatics. 2007; 8:381. [PubMed: 17931421]
16. Vavricka SR, Musch MW, Chang JE, Nakagawa Y, Phanvijhitsiri K, Waypa TS, Merlin D, Schneewind O, Chang EB. hPepT1 transports muramyl dipeptide, activating NF-κB and stimulating IL-8 secretion in human colonic Caco2/bbe cells. Gastroenterology. 2004; 127:1401–1409. [PubMed: 15521010]
17. Ismair MG, Vavricka SR, Kullak-Ublick GA, Fried M, Mengin-Lecreulx D, Girardin SE. hPepT1 selectively transports muramyl dipeptide but not Nod1-activating muramyl peptides. Canadian Journal of Physiology and Pharmacology. 2006; 84:1313–1319. [PubMed: 17487240]
18. Lee J, Tattoli I, Wojtal KA, Vavricka SR, Philpott DJ, Girardin SE. pH-dependent Internalization of Muramyl Peptides from Early Endosomes Enables Nod1 and Nod2 Signaling. J Biol Chem. 2009; 284:23818–23829. [PubMed: 19570976]
19. Dalmasso G, Nguyen HTT, Charrier-Hisamuddin L, Yan Y, Laroui H, Demoulin B, Sitaraman SV, Merlin D. PepT1 mediates transport of the proinflammatory bacterial tripeptide l-Ala-γ-d-Glu-meso-DAP in intestinal epithelial cells. 2010
20. Nakamura N, Lill JR, Phung Q, Jiang Z, Bakalarski C, de Maziere A, Klumperman J, Schlatter M, Delamarre L, Mellman I. Endosomes are specialized platforms for bacterial sensing and NOD2 signalling. Nature. 2014; 509:240–244. [PubMed: 24695226]
21. Charriere GM, Ip WE, Dejardin S, Boyer L, Sokolovska A, Cappillino MP, Cherayil BJ, Podolsky DK, Kobayashi KS, Silverman N, Lacy-Hulbert A, Stuart LM. Identification of Drosophila Yin and PEPT2 as evolutionarily conserved phagosome-associated muramyl dipeptide transporters. J Biol Chem. 2010; 285:20147–20154. [PubMed: 20406817]
22. Lim JH, Kim MS, Kim HE, Yano T, Oshima Y, Aggarwal K, Goldman WE, Silverman N, Kurata S, Oh BH. Structural basis for preferential recognition of diaminopimelic acid-type peptidoglycan by a subset of peptidoglycan recognition proteins. J Biol Chem. 2006; 281:8286–8295. [PubMed: 16428381]
23. Rees DC, Johnson E, Lewinson O. ABC transporters: the power to change. Nature reviews Molecular cell biology. 2009; 10:218–227. [PubMed: 19234479]
24. Hediger MA, Clémençon B, Burrier RE, Bruford EA. The ABCs of membrane transporters in health and disease (SLC series): Introduction. Molecular Aspects of Medicine. 2013; 34:95–107. [PubMed: 23506860]

25. Paquette N, Broemer M, Aggarwal K, Chen L, Husson M, Erturk-Hasdemir D, Reichhart JM, Meier P, Silverman N. Caspase-mediated cleavage, IAP binding, and ubiquitination: linking three mechanisms crucial for Drosophila NF-kappaB signaling. Mol Cell. 2010; 37:172–182. [PubMed: 20122400]

26. Kim CH, Paik D, Rus F, Silverman N. The caspase-8 homolog Dredd cleaves Imd and Relish but is not inhibited by p35. J Biol Chem. 2014; 289:20092–20101. [PubMed: 24891502]

27. McGettigan J, McLennan RKJ, Broderick KE, Kean L, Allan AK, Cabrero P, Regulski MR, Pollock VP, Gould GW, Davies SA, Dow JAT. Insect renal tubules constitute a cell-autonomous immune system that protects the organism against bacterial infection. Insect Biochem Mol Biol. 2005; 35:741–754. [PubMed: 15894191]

28. Celniker SE, Dillon LAL, Gerstein MB, Gunsalus KC, Henikoff S, Karpen GH, Kellis M, Lai EC, Lieb JD, MacAlpine DM, Micklem G, Piano F, Snyder M, Stein L, White KP, Waterston RH. Unlocking the secrets of the genome. Nature. 2009; 459:927–930. [PubMed: 19536255]

29. Qiu A, Jansen M, Sakaris A, Min SH, Chattopadhyay S, Tsai E, Sandoval C, Zhao R, Akabas MH, Goldman ID. Identification of an intestinal folate transporter and the molecular basis for hereditary folate malabsorption. Cell. 2006; 127:917–928. [PubMed: 17129779]

30. Kim MG, Flomerfelt FA, Lee KN, Chen C, Schwartz RH. A putative 12 transmembrane domain cotransporter expressed in thymic cortical epithelial cells. J Immunol. 2000; 164:3185–3192. [PubMed: 10706709]

31. Tigno-Aranjuez JT, Asara JM, Abbott DW. Inhibition of RIP2's tyrosine kinase activity limits NOD2-driven cytokine responses. Genes Dev. 2010; 24:2666–2677. [PubMed: 21123652]

32. Harder J, Núñez G. Functional Expression of the Intracellular Pattern Recognition Receptor NOD1 in Human Keratinocytes. Journal of Investigative Dermatology. 2009; 129:1299–1302. [PubMed: 19122645]

33. Magalhaes JG, Philpott DJ, Nahori MA, Jehanno M, Fritz J, Le Bourhis L, Viala J, Hugot JP, Giovannini M, Bertin J, Lepoivre M, Mengin-Lecreulx D, Sansonetti PJ, Girardin SE. Murine Nod1 but not its human orthologue mediates innate immune detection of tracheal cytotoxin. EMBO Rep. 2005; 6:1201–1207. [PubMed: 16211083]

34. Höglund PJ, Nordström KJV, Schiöth HB, Fredriksson R. The Solute Carrier Families Have a Remarkably Long Evolutionary History with the Majority of the Human Families Present before Divergence of Bilaterian Species. Mol Biol Evol. 2011; 28:1531–1541. [PubMed: 21186191]

35. Schlessinger A, Matsson P, Shima JE, Pieper U, Yee SW, Kelly L, Apeltsin L, Stroud RM, Ferrin TE, Giacomini KM, Sali A. Comparison of human solute carriers. Protein Sci. 2010; 19:412–428. [PubMed: 20052679]

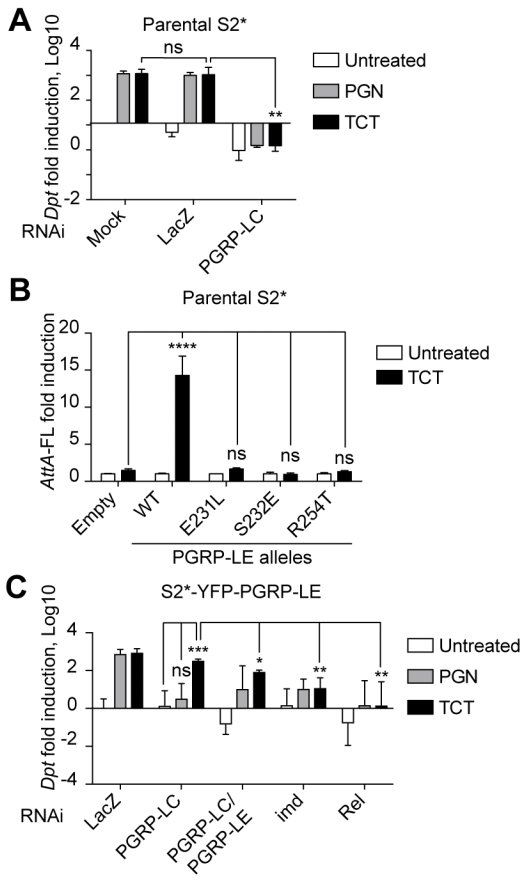

Figure 1.

Drosophila S2* cells present TCT to the cytosolic innate immune receptor PGRP-LE. (A) PGRP-LC RNAi blocked *Dpt* induction in S2* cells upon stimulation with either polymeric PGN or TCT. *Dpt* transcript was measured by qRT-PCR. (B) Upon TCT stimulation, *AttA*-luciferase activity increased only in S2* cells expressing wild type but not mutant PGRP-LE alleles. (C) S2* cells stably expressing YFP-PGRP-LE induced *Dpt* in response to TCT independent of *PGRP-LC*. Mean +/− SD from three or more biological replicates are presented. y-axes show Log_{10} *Dpt* fold-induction normalized to GAPDH1 (A, C) or firefly luciferase fold-induction normalized to a *Copia* Renilla luciferase reporter (B). ****; p<0.0001, ***; p<0.001, **; p<0.01, *; p<0.05, ns; not significant by Tukey's multiple comparison following 2-way ANOVA.

A

Uniprot ID	Gene_id	Other name	Closest human protein
Q9VHX9	CG2791	CD98hc	**SLC3A**
Q7KUL6	CG3297	Minidiscs	**SLC7A**
Q9VKC2	CG12317	JhI-21	**SLC7A**
P91679	CG2913	Yin	**SLC15A**
Q9VLM4	CG13384	MDR 4 ortholog	**SLC36A**
Q86P46	CG8046		**SLC46A**
Q8T9C5	CG6214	MDR-like protein 1	ABCC4
Q8T9B4	CG7627		ABCC4
Q9VGM1	CG14709		ABCC4
Q9VC63	CG5789		CFTR/ ABCC7
Q9VXR5	CG9281		ABCF2
Q8SZF5	CG3164		ABCG

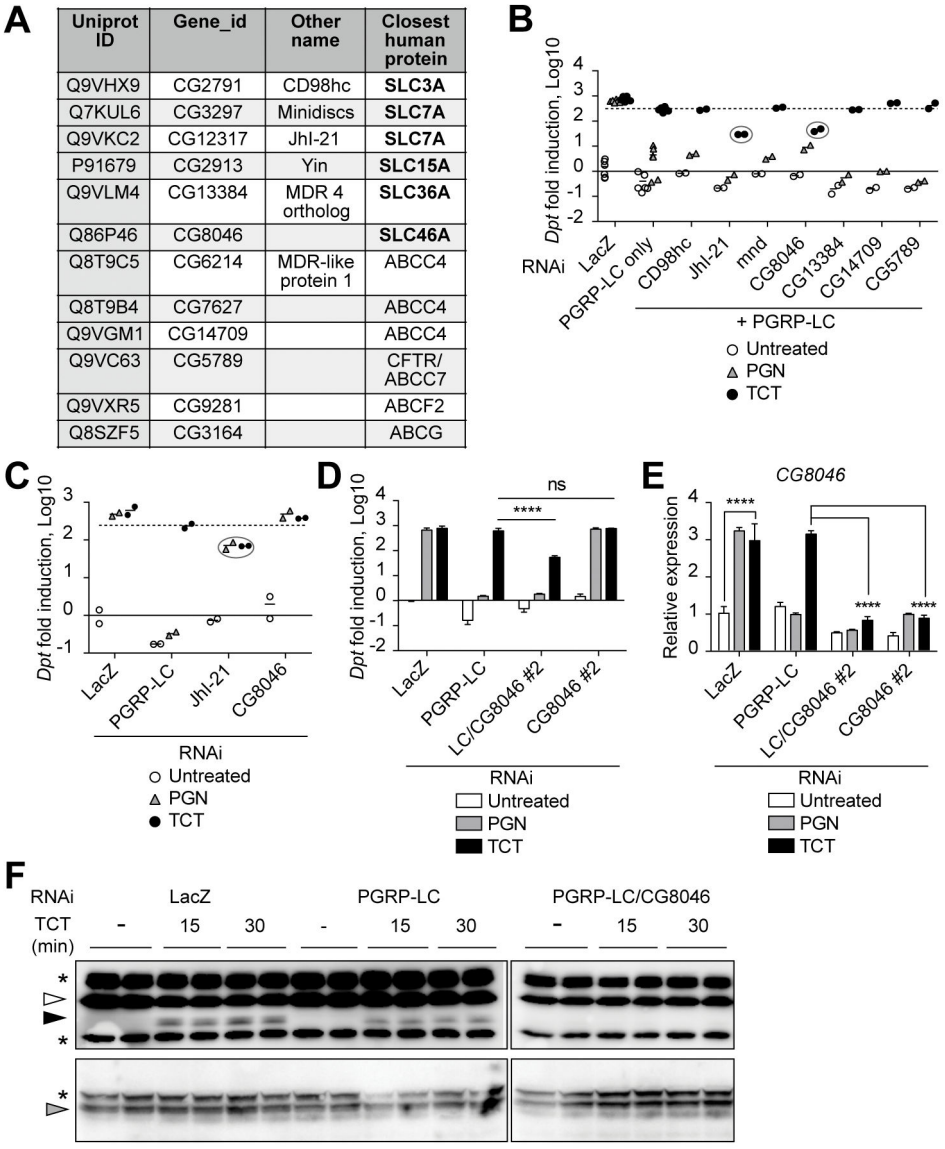

Figure 2.

CG8046 is required for cytosolic TCT recognition. (A) Transporter candidates identified from S2* cell phagosome by Charrière *et al.* (21). (B) RNAi targeting *JhI-21* or *CG8046* in combination with *PGRP-LC* significantly inhibited *Dpt* induction upon TCT stimulation (marked with gray circles). (C) CG8046 single knockdown did not affect *Dpt* induction triggered through PGRP-LC, while *JhI-21* RNAi still significantly impaired *Dpt* induction (marked with gray circles). (D) A distinct dsRNA targeting a different region in CG8046 significantly inhibited *Dpt* induction upon TCT stimulation of the cytosolic PGRP-LE pathway. (E) CG8046 knockdown efficiencies were greater than 60%, and *CG8046* expression is immune-inducible. All relevant data points and their means (B and C) or Mean −/+ SD from three biological replicates (D and E) are presented. y-axes show Log_{10} *Dpt* fold-induction normalized to GAPDH1 (B through D) or CG8046 expression normalized to GAPDH1. ****; p<0.0001, ***; p<0.001, **; p<0.01, ns; not significant by Tukey's

multiple comparison following 2-way ANOVA. (F) CG8046 functions upstream of Imd cleavage. TCT-triggered Imd cleavage was profoundly impaired with *PGRP-LC* and *CG8046* double knockdown compared to *PGRP-LC* single knockdown (top), while expression of YFP-PGRP-LE was unchanged (bottom). The blot was probed for Imd first and then stripped and reprobed with for YFP-PGRP-LE. White triangle; full-length Imd, black triangle; cleaved Imd, gray triangle: YFP-PGRP-LE, asterisk; non-specific.

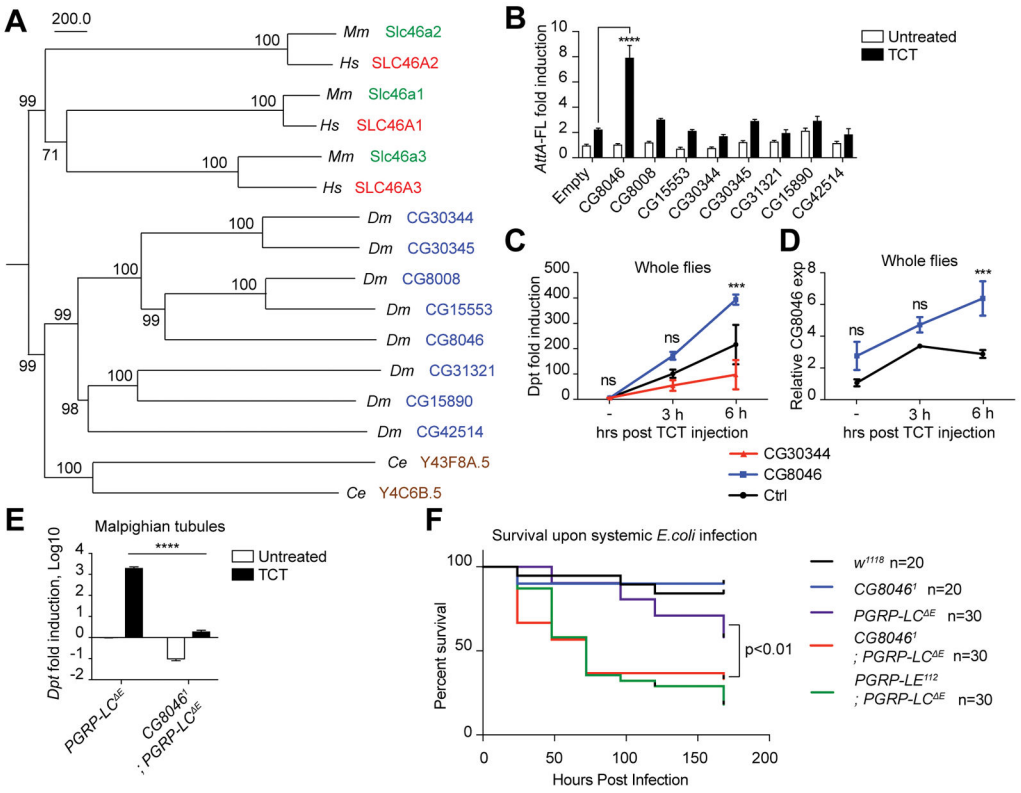

Figure 3.

CG8046 promotes TCT recognition *in vivo* and plays an important role in systemic protection against *E. coli* infection. (A) Phylogenetic tree of SLC46 homologs from human, mouse, *Drosophila* and *C. elegans*. (B) Cytosolic recognition, as assayed with *Attacin*-luciferase, revealed that overexpression of CG8046 significantly increased *AttA*-luciferase activity (empty vector vs CG8046), while six other *Drosophila* SLC46s were inactive. CG15553 was not expressed in these assays, see Supplement Figure 2A&B. (C, D) Overexpression of *CG8046* in the adult fat body enhanced TCT-stimulated *Diptericin* transcription. *Dpt* (C) and *CG8046* (D) expression were measured by qRT-PCR 3 h and 6 h after microinjection of TCT. (E) *Dpt* induction upon systemic TCT stimulation was significantly reduced in Malpighian tubules of *PGRP-LC, CG8046* double mutants. (F) Double mutant flies lacking both *PGRP-LC* and *CG8046* were susceptible to systemic *E. coli* infection, similar to *PGRP-LC, PGRP-LE* double mutant flies. y-axes show relative luciferase activity normalized to Renilla luciferase (B) or relative gene expression normalized to GAPDH1 (C, D and E). Mean +/− SD from three biological replicates are presented (B through E) and one representative assay, among 7 independent experiments, is presented (F). ****; p<0.0001, ***; p<0.001, **; p<0.01, *; p<0.05, ns; not significant by Tukey's multiple comparison following 2-way ANOVA (B through E) or log-rank test (F).

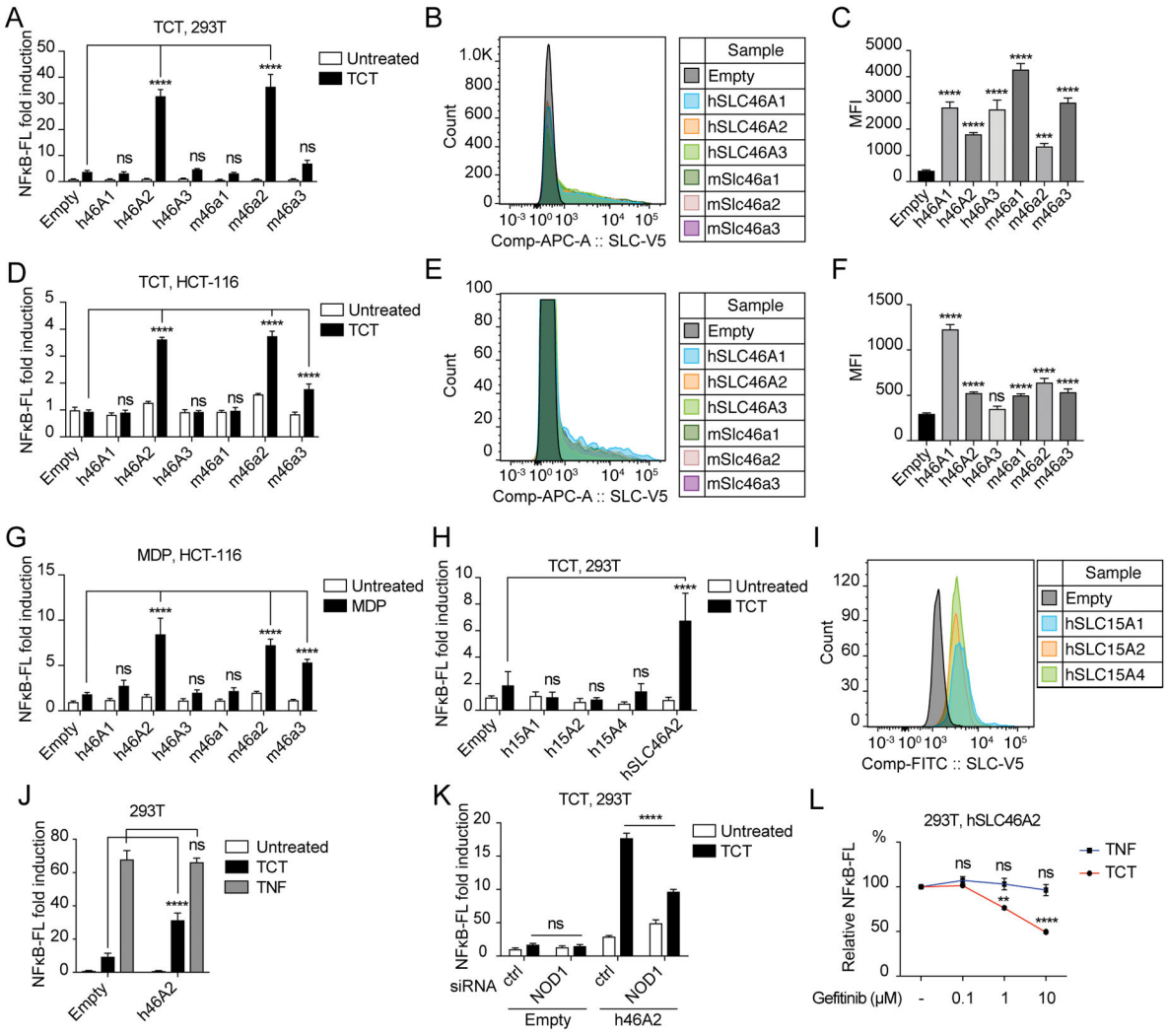

Figure 4.

Mammalian SLC46 transporters facilitate PGN recognition by NOD receptors. (A) NF-κB-luciferase assays in HEK293 cells transiently expressing human or mouse SLC46 homologs showed that human SLC46A2 and mouse Slc46a2 markedly enhanced in NF-κB activity upon TCT stimulation. (B, C) Expression of SLC46 transgenes in HEK293 cells was analyzed by flow cytometry of live, single cells stained with anti-V5 staining. Representative histograms were overlaid (B) and the mean fluorescence intensity from three independent transfections is presented (C). Expression of all SLC46 transgenes was comparable. (D) Dual-luciferase assays as in (A) were repeated in HCT-116 cells. A significant increase in NF-κB-luciferase activity was observed with human SLC46A2, mouse Slc46a2, and -a3 upon TCT stimulation. (E, F) Expression of SLC46 transgenes in HCT-116 cells was checked as in panel B and C by flow cytometry. Expression of all SLC46 transgenes was comparable except human SLC46A3 which was not significantly higher than empty vector control transfection. (G) Human SLC46A2, mouse Slc46a2 and -3 enhanced NF-κB luciferase activity in response to MDP in HCT-116 cells. (H, I) SLC15A1, A2 and A4 did not support NF-κB activation in response to TCT in HEK293 cells. Expression of SLC15

transgenes in HEK293 cells was analyzed by flow cytometry. (J) SLC46A2 did not enhance NF-κB activation in response to TNF in HEK293 cells. (K) TCT-activated, SLC46A2 facilitated NF-κB activation is NOD1-dependent, as NOD1 RNAi significantly blocked NF-κB activation compared to a non-targeting control. (L) Gefitinib, a RIP2 tyrosine kinase inhibitor, inhibited NF-κB activity upon TCT stimulation but not upon TNF in HEK293 cells expressing SLC46A2. Mean +/− SD from three biological replicates are presented. ****; $p<0.0001$, ***; $p<0.001$, ns; not significant by Tukey's multiple comparison following 2-way ANOVA.

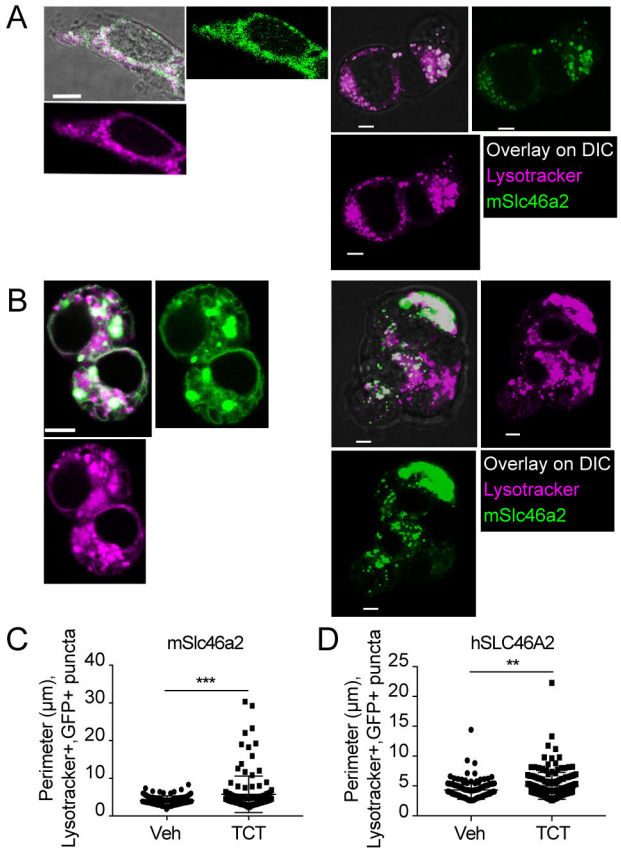

Figure 5.

Confocal microscopy reveals that SLC46A2-EGFP clusters in response to TCT. HEK-293T cells were transfected with SLC46A2-EGFP, and exposed to LysoTracker (magenta). (A) mSlc46a2-EGFP (green) is evenly distributed and co-localized with LysoTracker-positive organelles throughout the cytoplasm without TCT. 2 representative images from independent assays, exhibiting the range of patterns of observed. (B) After 30-minute exposure to TCT, mSlc46a2-EGFP-expressing, LysoTracker-positive organelles relocalized to form large aggregates. (C) Sizes of $EGFP^{+}$ and $Lysotracker^{+}$ puncta were measured and compared in the absence of TCT (n=110 puncta from of 13 cells) or presence of TCT (n=129 puncta from 21 cells) from two independent assays. (D) Human SLC46A2-EGFP protein showed similar behavior as its mouse homolog upon TCT exposure (n=137 puncta from 30 cells for vehicle, n=173 puncta from 35 cells for TCT). All data points are presented, and the mean is indicated. ** $p < 0.01$, *** $p < 0.001$, unpaired two-tailed t-test. For all images, the scale bar is 5 µm.